Structure–activity relationship for extracellular block of K+ channels by tetraalkylammonium ions

Victor B. Luzhkov, Fredrik Österberg, Johan Åqvist*

Department of Cell and Molecular Biology, Uppsala University, BMC, Box 596, SE-751 24 Uppsala, Sweden

Abstract **External tetraalkylammonium ion binding to potassium channels is studied using microscopic molecular modelling methods and the experimental structure of the KcsA channel. Relative binding free energies of the KcsA complexes with Me_4N^+, Et_4N^+, and n-Pr_4N^+ are calculated with the molecular dynamics free energy perturbation approach together with automated ligand docking. The four-fold symmetry of the entrance cavity formed by the Tyr82 residues is found to provide stronger binding for the D_{2d} than for the S_4 conformation of the ligands. In agreement with experiment the Et_4N^+ blocker shows several kcal/mol better binding than the other tetraalkylammonium ions.**
© 2003 Published by Elsevier B.V. on behalf of the Federation of European Biochemical Societies.

Key words: Potassium channel; Blocking; Tetraethylammonium; Free energy calculation; Molecular dynamics

1. Introduction

Studies of ion current blocking (inhibition) in potassium channels provide useful and informative clues for understanding the biophysics and pharmacology of these important and ubiquitous membrane proteins (see, e.g. [1–3]). Structurally, potassium ion channels present complex pores in biological membranes and a common mechanism of blocking involves binding of small or medium sized blocker molecules at the ion permeation path. The recently determined X-ray structures of several bacterial K+ channels [4–6] provide an important basis for mechanistic studies of the potassium channel blockade. A well-known type of blockers are the quaternary ammonium ions (QAIs), which are frequently used as molecular probes in exploring the functionality of K+ channels [1,7–10]. Already early experimental studies showed a marked efficacy of extracellular application of tetraethylammonium ion, Et_4N^+ (TEA), in K+ channel blockade [8] where the important role of four aromatic residues, corresponding to Y82 in KcsA, was later detected [1,11–15].

The blockade of KcsA by TEA has recently been addressed in several molecular modelling studies [16–18]. In our earlier work [16], binding of the two low-energy TEA conformations, D_{2d} and S_4, (denoted TEA2 and TEA1 in [16], respectively), was explored using automated docking and molecular dynamics (MD) simulations where binding energies were examined using the linear interaction energy (LIE) method [19,20]. The binding modes at the external and internal blocking sites were considered and the predicted structure of the internal TEA complex agrees very well with the subsequently reported X-ray structure of KcsA with a tetrabutylammonium analog [21]. Regarding the external binding, our work [16] demonstrated the importance of hydrophobic interactions between the ligand and the tyrosine residues Y82, and further showed that the Y82V mutations substantially reduce the binding affinity for TEA. The absolute binding free energies of the TEA complexes with KcsA, which were estimated in [16] from the MD trajectories using the LIE method, were also in reasonable agreement with experimental results [14,15]. However, the issue of whether the D_{2d} or S_4 blocker conformation is favored still remains unresolved. While results from the AutoDock scoring function [22] indicate that the D_{2d} conformer has the highest affinity at the external site [16,18], our MD/LIE calculations favored the S_4 conformer, at least if partial insertion of one of the ethyl groups into the first filter position was allowed. However, there is yet no work that has evaluated the energetics of external D_{2d} vs. S_4 binding for the filter loading state that is predicted to be most stable [23] by rigorous free energy calculations.

The purpose of the present work is to explore structure–activity relationships for a series of QAIs that bind to the external entrance cavity in KcsA. In order to resolve questions regarding the exact binding mode it is clearly more reliable to examine a series of related compounds, for which there is experimentally a non-trivial binding optimum, rather than to just focus on a single compound. Furthermore, this is a case where accurate free energy perturbation (FEP) simulations can be employed based on force fields (FFs) that have been verified to reproduce the solution properties of the blockers [24]. It should also be kept in mind that the structure of the bacterial KcsA channel is considered as a template for many mammalian potassium channels as well, and it is therefore of considerable interest to understand the structure–activity relationships behind blocking. The binding free energies of KcsA complexes with Me_4N^+ (TMA), Et_4N^+ (TEA), and n-Pr_4N^+ (TPrA) are thus calculated herein using a combination of automated docking and FEP/MD computational techniques.

2. Materials and methods

The binding of QAIs to the external entrance of the KcsA pore is explored in several steps. First, the structures of the channel–blocker

*Corresponding author. Fax: (46)-18-536971.
E-mail address:* johan.aqvist@icm.uu.se (J. Åqvist).

complexes are obtained from automated docking, and the generated structures are then subjected to equilibration by MD simulations. Finally, the relative binding energies of the QAIs are estimated using the microscopic FEP/MD approach. The latter method is based on Zwanzig's equation [25] for calculating the free energy difference between states of interest and presents one of the most reliable ways of evaluating free energies of ligand binding from computer simulations [26,27].

The MD calculations are carried out with the all-atom Amber-95/ TIP3P [28] FF for ammonium ions, protein and water molecules using the program Q [29]. The closed KcsA (1bl8) crystal structure [4] with E71 side chains according to [30] (that agrees perfectly with the subsequently published higher resolution structure 1k4c) was used as the starting structure. The automated docking is performed with the united-atom Amber-type FF using the program AutoDock3.0 [22]. The previously reported RESP PCM/HF/6-31G(d) atomic charges of QAIs [24] are used in both methods. The docking of QAIs is performed with pre-selected conformations (either D_{2d} or S_4) at the quaternary center. The docked ligand positions are determined for the rigid experimental structure of KcsA and the filled channel pore (state 0101, see below). The simulation system in the MD calculations consists of the KcsA–ligand complex surrounded by a model membrane [23,30] and a 25.0 Å radius sphere of water molecules. Protein atoms outside the 25 Å sphere were restrained to their crystallographic positions by a 100 kcal/(mol Å²) force constant, while those inside the shell between 22 and 25 Å are subject to a weaker 10 kcal/(mol Å²) restraint and atoms within 22 Å of the center move freely. A constant temperature of 300 K was maintained by standard coupling to a thermal bath [38]. Simulations of the free ligands in aqueous solution are also done within a water sphere of the same size. The center of the water sphere for the ligand–channel complexes is placed at the position of the first ion binding site (the site closest to the extracellular channel entry) in the selectivity filter. The lowest energy occupancy state (0101) of the selectivity filter is considered in the MD and docking calculations, according to the proposed potassium channel permeation mechanism [23,30]. In this state the channel pore contains two water molecules in the first and the third ion binding sites, and K^+ ions in the second and the fourth ion binding sites of selectivity filter. The central cavity ion which is over 20 Å away from the blocker binding site was not included in the simulations. The total charge of the channel is taken to be zero. Although long-range electrostatics is taken care of as in [23,30], one can note that the calculation of relative binding energies, where no net charges are created or annihilated, presents a much simpler problem than calculation of absolute free energies. Other details for setting up the MD and automated docking calculations are explained in our previous works [16,30].

The FEP procedure for calculation of relative ligand binding energies involves the use of the standard thermodynamic cycle in Fig. 1, where chemical transformations (mutation) between the QAIs are performed in the channel–blocker complexes and in aqueous solution. The closure of the cycle gives the expression for the relative binding energy, $\Delta\Delta G_{bind}$, of two ligands, A and B.

$$\Delta\Delta G_{bind}(B-A) \equiv \Delta G_{bind}(B) - \Delta G_{bind}(A) = \Delta G_{mut}^{prot} - \Delta G_{mut}^{wat} \quad (1)$$

The relative hydration energies, $\Delta\Delta G_{sol}(B-A) \equiv \Delta G_{sol}(B) - \Delta G_{sol}(A)$, are calculated in a similar way by considering the corresponding cycle for ligand mutations in water and vacuum. The free energies of the ligand transformation $A \rightarrow B$ (Eq. 1) in the channel complex, ΔG_{mut}^{prot}, and in water, ΔG_{mut}^{wat}, are evaluated from microscopic FEP/MD calculations based on extensive sampling of the system configurational space during gradual transformation between the states of interest (see, e.g. discussion of the method given elsewhere [26,27]). In the FEP protocol the potential surfaces of initial and final states of the model system are 'connected' via a set of intermediate mapping potentials. The free energy associated with the transformation from the potential ε_A to ε_B in n discrete steps is obtained as a sum over the averages $\langle\rangle_m$ evaluated from the thermodynamic ensembles for the potential surfaces ε_m

$$\Delta G(A \rightarrow B) = \Delta G(\vec{\lambda}_1 \rightarrow \vec{\lambda}_n) =$$

$$-RT \sum_{m=1}^{m=n-1} \ln\langle\exp[-(\varepsilon_{m+1}-\varepsilon_m)/RT]\rangle_m \quad (2)$$

where $\varepsilon_m = \lambda_A^m \varepsilon_A + \lambda_B^m \varepsilon_B$.

The mapping vector $\vec{\lambda}_m = (\lambda_A^m, \lambda_B^m)$ changes between the values (1,0) and (0,1) for the initial and final states, respectively, with the constraint $\lambda_A^m + \lambda_B^m = 1$. The sum in Eq. 2 is calculated as an average for summation in the forward and backward directions. The difference of the latter two values is one of the criteria of FEP convergence. In the cases, when the ligand mutations include changes in chemical bond lengths, use of the harmonic approximation for bond energy terms in Eq. 2 frequently gives poor convergence due to large energy fluctuations in these terms. The FEP convergence is substantially improved by using SHAKE constraints [31] on mutated chemical bonds. However, in this case $\Delta G(A \rightarrow B)$ of Eq. 2 does not contain the potential of mean force contributions from the bond terms. This type of free energy contribution, ΔG_{xp}, which originates from the constrained bond transformations can, however, be evaluated by considering uncoupled mutations of the FF parameters, ε, and the atomic coordinates, R, in each $\vec{\lambda}_m$ step of the mapping procedure [32,33].

$$\Delta G_{xp}(\vec{\lambda}_m \rightarrow \vec{\lambda}_{m+1}) = \Delta G(\varepsilon_m, R_m \rightarrow \varepsilon_m, R_{m+1}) \quad (3)$$

$$\Delta G_{tot}(\vec{\lambda}_m \rightarrow \vec{\lambda}_{m+1}) = \Delta G(\varepsilon_m, R_m \rightarrow \varepsilon_m, R_{m+1})$$

$$+\Delta G(\varepsilon_m, R_{m+1} \rightarrow \varepsilon_{m+1}, R_{m+1}) \quad (4)$$

The total free energy difference between the states of interest, $\Delta G_{tot}(A \rightarrow B)$ in Eq. 4, is given here essentially as the sum of $\Delta G(A \rightarrow B)$ from Eq. 2 and $\Delta G_{xp}(A \rightarrow B)$ from Eq. 3. The significance and implementation of the coordinate-coupled contribution, ΔG_{xp}, in the FEP protocol has been discussed earlier [33,34], and this term is explicitly evaluated in the present work.

The studied mutations of QAI structure involve gradual changing of the end methyl groups, -CH_3, to hydrogens, -Hd_3, where d denotes a dummy atom with zero values of non-bonded parameters. The $C \rightarrow H$ and $H \rightarrow d$ transformations of atom types in the molecular topology define changes in the corresponding FFs. The single-topology description of mutated system is used. Transformations of QAI structures are performed only in the direction of 'shrinking' the molecule in order to produce mutation paths just for the single pre-selected conformation at the quaternary center. We use the Amber-95 atom types N3, CT, and HP [28] for all QAIs. The H–d bond length (0.6 Å) is taken shorter than the C–H bond length (1.09 Å) to avoid sampling problems at the end points of transformations. The C–N bond length is 1.510 Å, and the C–C bond length is 1.526 Å according to the results of ab initio calculations for the considered QAIs [24].

The FEP/MD calculations are performed using a 100–200 ps equilibration phase and approximately 400 ps mutation phase. In the course of mutations, the electrostatic terms are first changed in 53 discrete steps, whereafter the intramolecular and non-bonded terms are transformed in 81 discrete steps. No positional restraints are applied to the ligands and channel atoms within the simulations sphere during the mutations. All bond lengths are constrained using the SHAKE procedure. The $\vec{\lambda}_m$ values are interspaced for optimal sampling efficiency [27]. The calculation at each value of $\vec{\lambda}_m$ includes 0.5 ps MD of initial equilibration and 2.5 ps MD for data collection, from which the free energies are calculated. The free energy associated with coordinate perturbations is calculated for mutation legs where the bond lengths are changed. The FEP/MD trajectories are calculated at a constant temperature of 300 K and a time step of 2 fs. Convergence errors in the trajectory sampling are estimated by comparing the free energies from the forward and backward summation in Eq. 2 and the results from several different MD trajectories. In addition we have run a series of forward and backward $Me_4N^+ \rightarrow K^+$ mutations, that do not suffer from the conformational D_{2d} vs. S_4 problem, to assess the FEP convergence errors. These different estimates all give an error range of ± 0.6 to ± 0.8 kcal/mol.

3. Results

3.1. Automated docking and MD simulations of the channel–ligand complexes

The structural features of the extracellular binding site for tetraalkylammonium ions in potassium channels have become clear from the X-ray studies of the bacterial KcsA channel [4,5]. This tetrameric structure reveals the presence of a bowl-
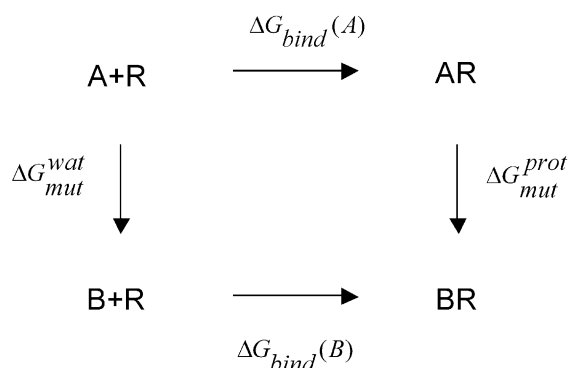
Fig. 1. Thermodynamic cycle for calculating relative ligand binding free energies.

shaped cavity at the outer entrance to the narrow selectivity filter. Unlike the transmembrane helices, which might change positions upon channel gating, the part of the channel near the selectivity filter is viewed as fairly rigid. The indicated site contains four aromatic phenyl rings of the Y82 residues, which form a symmetric hydrophobic cage (Fig. 2). Moreover, the surface of this site is lined with the backbone oxygen atoms of Y78 and G79, as illustrated in Fig. 2. Such a structure apparently provides an amphiphilic character for the outer channel vestibule and allows efficient binding of both small permeant cations and larger hydrophobic ions. The X-ray study [5] indeed shows a position for K^+ in the center of the external cavity of KcsA under high ion concentration. This position, in fact, agrees precisely with that predicted earlier for the central nitrogen atom of TEA in [16]. Experimental measurements show that the binding affinities of QAIs increase in the order: $Me_4N^+ < n\text{-}Pr_4N^+ < Et_4N^+$ (Table 1), where the Et_4N^+ dissociation constant is in the range of 0.01–1 mM.

The automated docking calculations show that both Me_4N^+, Et_4N^+ and the even larger $n\text{-}Pr_4N^+$ can be snugly accommodated at the external binding site of KcsA. The docked position for the small Me_4N^+ lies near one of the four Y82 residues, in which case the nitrogen atom is displaced away from the channel symmetry axis. The docked Et_4N^+ and $n\text{-}Pr_4N^+$ ions find positions in the central part of the outer cavity between the Y82 phenyl rings. The fourfold symmetry of the binding site favors binding of the D_{2d} conformers rather than S_4 according to the AutoDock scoring
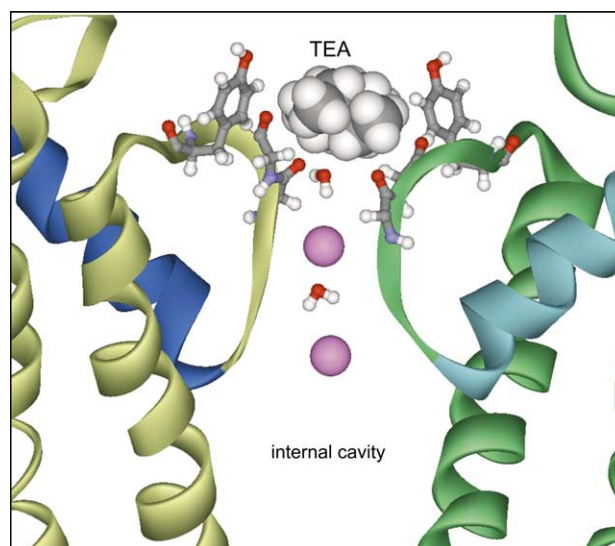

Fig. 2. Structure of the KcsA–D_{2d} TEA complex showing an instantaneous snapshot of the channel–ligand complex after 600 ps of MD. The ligand is shown as a space-filling model. The O atoms of the Y78, G79 and Y82 residues are shown in red and the K^+ atoms in the channel pore as colored (magenta) spheres. Only two out of four channel monomers are displayed.

function, as noted earlier [16,18]. However, the strongest binding in the docking calculations is predicted for D_{2d} $n\text{-}Pr_4N^+$ rather than for Et_4N^+ (Table 1).

The docked structures of the channel–blocker complexes were further explored using microscopic MD simulations. In the MD trajectories of the KcsA–Me_4N^+ complex the ligand fills only part of the 'tyrosine cage' space, and its position is subject to substantial variations. In this case the ligand drifts inside the outer vestibule and interacts with different pairs of Y82 residues. The ligand positions remain stable in MD trajectories for the channel complexes with Et_4N^+ (Figs. 2 and 3) and $n\text{-}Pr_4N^+$. Trajectory analysis for D_{2d} Et_4N^+ shows that, despite the fairly good match of the shape, the ligand does not have an entirely rigid position in the outer binding site. This is seen from partial rotations of the host Y82 phenyl rings to maximize the contact surface with the ligand. Moreover, the D_{2d} Et_4N^+ trajectory indicates the possibility of ligand tumbling within the binding site, while the overall structure of the channel–ligand complex is preserved (Fig. 3). It is worth mentioning in this respect our earlier observation that the D_{2d}

Table 1
Experimental binding data and results from automated docking calculations for the external complexes of tetraalkylammonium ions with potassium channels

Method	K^+ channel	QAI		
		Me_4N^+	Et_4N^+	$n\text{-}Pr_4N^+$
Experiment	Shaker H4, T449Y [11][a]	–	0.59	–
	rKv 1.1 [35][b]	–	0.36	–
	Kv 3.1 [9][b]	65	0.085	1.2
	Kv 3.1 [9][b]	45	0.056	2.4
	Shaker B, T449Y [9][b]	234	0.48	36
	KcsA [14][a]	–	3.2	–
	KcsA [15][a]	300	2.0	50
AutoDock3.0	KcsA[c]	−3.0	−5.1 (D_{2d})	−5.5 (D_{2d})
			−4.6 (S_4)	−5.0 (S_4)

[a]IC_{50} (mM).
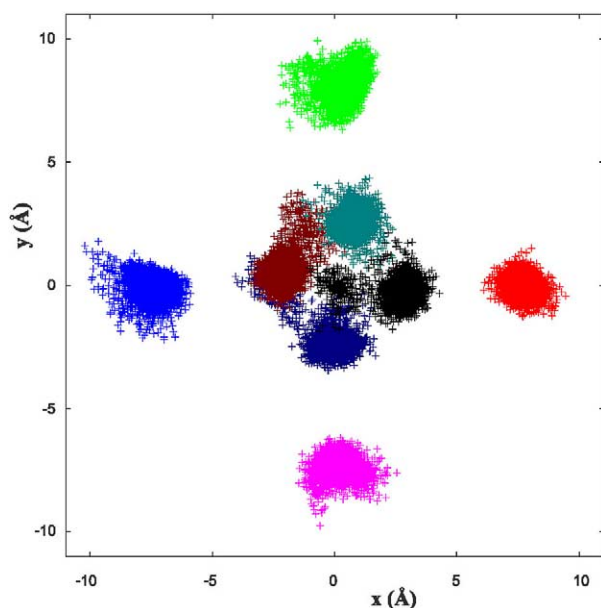[b]K_d (mM).
[c]ΔG_{bind} (kcal/mol).

Fig. 3. Instantaneous positions (in Å) in the plane perpendicular to the channel axis of the D_{2d} TEA end carbon atoms (inner four colors) and CZ carbon atoms of four Y82 phenol groups (outer four colors). A 1000 ps trajectory after 100 ps of equilibration is depicted.

conformation in the external KcsA–Et_4N^+ complexes can undergo transitions to the S_4 conformation in long MD trajectories that used the Gromos-87 potential. This may be related to the relatively small torsional barrier about the C–N bond in the Gromos-87 FF. In contrast, the all-atom Amber-95 FF calculations predict conformational stability of the D_{2d} and S_4 structures for both Et_4N^+ and n-Pr_4N^+ in the external binding site. In the D_{2d} n-Pr_4N^+ complex the ligand is partially rotated out of the binding site plane in such a way that one of the alkyl groups escapes the steric clash with the adjacent phenyl ring. The average position of the quaternary nitrogen atom in the D_{2d} n-Pr_4N^+ complex is shifted ∼0.5 Å outwards from the channel entrance compared to the D_{2d} Et_4N^+ complex.

3.2. FEP/MD calculations of binding energies

The structural transformations of QAIs in the FEP/MD calculations are performed in vacuum, water and channel complexes which allows us to evaluate the relative free energies of solvation $\Delta\Delta G_{sol}$, and binding, $\Delta\Delta G_{bind}$, according to the thermodynamic cycle in Fig. 1. Two successive transformations of QAIs are examined, n-$Pr_4N^+ \rightarrow Et_4N^+$ and $Et_4N^+ \rightarrow Me_4N^+$ (Fig. 4). The particular one-way direction of mutations is selected to preserve the specified conformation of the ligand, i.e. either D_{2d} or S_4. The conformation at the quaternary nitrogen center is conserved in all simulations due to the high interconversion barriers, which is ∼10 kcal/mol in Et_4N^+ [24]. The calculated relative binding free energies are given in Table 2.

The absolute values of solvation free energies, ΔG_{sol}, of the blockers increase when the size of the ammonium ion becomes smaller. The experimental relative solvation energies for n-$Pr_4N^+ \rightarrow Et_4N^+$ and $Et_4N^+ \rightarrow Me_4N^+$ are −2.5 and −7.5 kcal/mol, respectively [24]. The FEP/MD values calculated here of $\Delta\Delta G_{sol}$ for the n-$Pr_4N^+ \rightarrow Et_4N^+$ mutation are
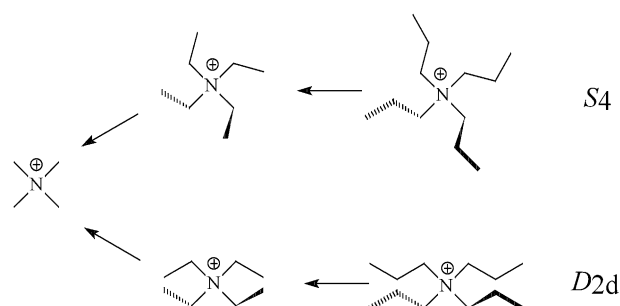

Fig. 4. Schematic pathways for the QAI transformations in FEP calculations.

−2.7±0.3 kcal/mol for D_{2d} and −3.1±0.5 kcal/mol for S_4 conformation. The calculated $\Delta\Delta G_{sol}$ for the $Et_4N^+ \rightarrow Me_4N^+$ mutation are −7.9±0.3 for D_{2d} and −8.2±0.5 kcal/mol for S_4 conformation. Thus the D_{2d} and S_4 conformations of QAIs have approximately equal hydration energies, with S_4 being slightly better solvated. The present results are in very good agreement with our earlier studies of QAI hydration using PCM/HF, PCM/DFT methods and FEP/MD simulations with different FFs [16,24]. The earlier reported theoretical and nuclear magnetic resonance (NMR) results predict that the D_{2d} and S_4 conformations of TEA have rather similar energies and may both exist in water solution [24], which agrees with other experimental data [36].

The results from FEP/MD calculations utilizing the thermodynamic cycle in Fig. 1 show that the D_{2d} conformation of Et_4N^+ binds stronger than the smaller Me_4N^+ ion by 2.4 kcal/mol and stronger than the larger D_{2d} n-Pr_4N^+ ion by 1.6 kcal/mol (Table 2). These values are in excellent agreement with experimental results. Considering the S_4 path in the ligand mutation scheme (Fig. 4), we find that Et_4N^+ binds better than n-Pr_4N^+ but worse than Me_4N^+. The ranking of $\Delta\Delta G_{bind}$ for the S_4 mutation path therefore apparently disagrees with the experimental observations. Upon examining the contributions to $\Delta\Delta G_{bind}$, one can see that the major effect as expected comes from the non-polar energy terms (nonpol) and xp in Table 2, while changes in the electrostatic (pol) contribution are small. The calculated energies also allow us

Table 2
Relative binding free energies (kcal/mol) of QAIs to the external binding site of KcsA

Mutation[a]		$Et_4N^+ \rightarrow Me_4N^+$		n-$Pr_4N^+ \rightarrow Et_4N^+$	
		Water	Channel	Water	Channel
S_4	pol	−42.59	−42.48	−6.78	−6.71
	nonpol	−11.93	−11.87	2.04	2.58
	xp	2.64	1.12	−1.63	−2.99
	tot	−51.88	−53.23	−6.37	−7.12
	$\Delta\Delta G_{bind}$[b]		−1.35		−0.75
D_{2d}	pol	−42.59	−42.68	−6.76	−6.80
	nonpol	−11.54	−9.11	2.68	3.59
	xp	2.78	2.88	−1.72	−4.26
	tot	−51.35	−48.91	−5.83	−7.47
	$\Delta\Delta G_{bind}$[b]		2.44		−1.64
Expt.	$\Delta\Delta G_{bind}$[c]		3.0		−1.9

[a]Pol is the electrostatic contribution, nonpol is the non-polar contribution (Eq. 4) and xp is the coordinate-coupling contribution (Eq. 3).
[b]Calculated using Eq. 4 as an average over three to six independent MD trajectories. The typical error bar is 0.6 kcal/mol.
[c]Calculated from IC_{50} values [15].

to estimate the relative binding energies of the D_{2d} and S_4 conformations of QAIs. This is done using Me_4N^+ as a common reference compound for both types of conformations in Fig. 4. Thus we obtain using Table 2 that the D_{2d} Et_4N^+ conformer binds better than S_4 Et_4N^+ by 3.8 kcal/mol, and that D_{2d} n-Pr_4N^+ binds better than S_4 n-Pr_4N^+ by 2.9 kcal/mol. These values can be compared with the absolute binding energies (calculated using K_d and IC_{50} values from Table 1), which are in the range from -3.4 to -5.6 kcal/mol for Et_4N^+ and from -1.8 to -4.0 kcal/mol for n-Pr_4N^+. If one assumes that the experimental values describe the D_{2d} binding, one can see that the S_4 conformation of these QAIs binds at the outer site only with low affinity in the stable 0101 loading state of the channel filter.

4. Discussion

We have reported results of molecular modelling of external complexes of the KcsA channel with the tetraalkylammonium ions Me_4N^+, Et_4N^+ and n-Pr_4N^+ in the D_{2d} and S_4 conformations. The position of the ligands in the channel complexes is predicted to be between the four Y82 residues near the selectivity filter entrance (Fig. 3), which agrees with amino acid mutation studies [11–15]. All three blockers can fit the binding site according to the docking calculations. This shows that despite the common view that the outer cavity precisely matches TEA binding, the volume of the site indeed also allows binding of larger ions. There is, in fact, no contradiction in a loose fit of Et_4N^+ to the outer channel cavity, since the binding affinities for Et_4N^+, and $PrEt_3N^+$ and $Pr_2Et_2N^+$ have been reported to be similar [9] which would seem to reflect an available volume that is somewhat larger than TEA.

The microscopic FEP/MD calculations, based on the all-atom Amber-95 FF, predict the ranking of binding free energies in very good agreement with experimental data (Table 2). Most important is the correctly predicted binding optimum for Et_4N^+. The docking calculations, on the contrary, incorrectly place the binding optimum for the D_{2d} conformation of n-Pr_4N^+, i.e. the ligand, which forms the most sterically tight complex. The present simulations now allow us to address the question of ligand binding conformation, which has not been resolved by experiments. QAIs exist in two major conformations, D_{2d} and S_4, where the former is more stable by 0.6–1.0 kcal/mol in solution [24] (note, that the prevalence of D_{2d} over S_4 in water was overestimated by a factor of ~ 5 in [17]). The QAIs also display conformational variations in crystalline molecular complexes, where the D_{2d} and S_4 conformations are observed in the ratio of 4:1 [37]. Comparing the FEP/MD data for the D_{2d} and S_4 conformations we can reliably discern the binding modes, where QAIs substitute for water molecules and possibly an ion in the outer binding site. The FEP/MD values of $\Delta\Delta G_{bind}$ for the D_{2d} conformer of QAIs explain all the experimental results, while the complexes of the S_4 conformers show a too small binding affinity. In fact, our earlier MD/LIE calculations also showed only a low affinity of the pyramidal S_4 conformation when the second and fourth filter sites were occupied by ions [16]. The corresponding affinities of external TEA to loading states that did not have an ion in the first two filter positions was found to be stronger, but these states are presumably too high in energy [23] to compete with the binding mode found herein.

The binding optimum for D_{2d} Et_4N^+ was also obtained

recently by us in preliminary FEP/MD simulations of QAI binding using harmonic potentials for the bond terms [27]. However, those calculations showed worse convergence than the present ones that use the SHAKE procedure and explicitly estimate the additional coordinate-coupling contribution to the FEP energies. The FEP energy contributions in Table 2 indicate that stabilization of the Et_4N^+ complexes, compared to the Me_4N^+ and n-Pr_4N^+ blockers, originates from the van der Waals and steric response of the binding site whereas electrostatic contributions to the differential binding energies are small. While such a decomposition, in principle, depends on the chosen mutation paths, the result that shape is the major determinant of selectivity here is quite natural. Cation-π effects that are, in fact, reasonably well represented in the Amber-95 FF, do not appear to play a major role in binding. Instead, for the absolute binding affinities the polar interactions are significant [16] and, as discussed earlier [16], it is a combination of this contribution and hydrophobic (non-polar) interactions that are important for stabilization of tetraalkylammonium ions at the external binding site.

References

[1] Hille, B. (1992) Ionic Channels of Excitable Membranes, Sinauer Associates, Sunderland, MA.
[2] Robertson, D.W. and Steinberg, M.I. (1990) J. Med. Chem. 33, 1529–1541.
[3] Coghlan, M.J., Carrol, W.A. and Gopalakrishnan, M. (2001) J. Med. Chem. 44, 1627–1653.
[4] Doyle, D.A., Cabral, J.M., Pfuetzner, R.A., Kuo, A., Gulbis, J.M., Cohen, S.L., Chait, B.T. and MacKinnon, R. (1998) Science 280, 69–77.
[5] Zhou, Y., Morais-Cabral, J.H., Kaufman, A. and MacKinnon, R. (2001) Nature 414, 43–48.
[6] Jiang, Y., Lee, A., Chen, J., Ruta, V., Cadene, M., Chait, B.T. and MacKinnon, R. (2003) Nature 423, 33–41.
[7] Armstrong, C.M. (1971) J. Gen. Physiol. 58, 413–437.
[8] Armstrong, C.M. and Hille, B. (1972) J. Gen. Physiol. 59, 388–400.
[9] Jarolimek, W., Soman, K.V., Alam, M. and Brown, A.M. (1996) Mol. Pharmacol. 49, 165–171.
[10] del Camino, D., Holmgren, M., Liu, Y. and Yellen, G. (2000) Nature 403, 321–325.
[11] MacKinnon, R. and Yellen, G. (1990) Science 250, 276–279.
[12] Kavanaugh, M.P., Varnum, M.D., Osborne, P.B., Christie, M.J., Busch, A.E., Adelman, J.P. and North, R.A. (1991) J. Biol. Chem. 266, 7583–7587.
[13] Heginbotham, L. and MacKinnon, R. (1992) Neuron 8, 483–491.
[14] Heginbotham, L., LeMsurier, M., Kolmakova-Partensky, L. and Miller, C. (1999) J. Gen. Physiol. 114, 551–559.
[15] Meuser, D., Splitt, H., Wagner, R. and Schrempf, H. (1999) FEBS Lett. 462, 447–452.
[16] Luzhkov, V.B. and Åqvist, J. (2001) FEBS Lett. 495, 191–196.
[17] Crouzy, S., Bernèche, S. and Roux, B. (2001) J. Gen. Physiol. 118, 207–216.
[18] Guidoni, L. and Carloni, P. (2002) J. Recept. Signal Transduct. 22, 315–331.
[19] Åqvist, J., Medina, C. and Samuelsson, J.E. (1994) Protein Eng. 7, 385–391.
[20] Åqvist, J., Luzhkov, V.B. and Brandsdal, B.O. (2002) Acc. Chem. Res. 35, 358–365.
[21] Zhou, M., Morais-Cabral, J.H., Mann, S. and MacKinnon, R. (2001) Nature 411, 657–661.
[22] Morris, G.M., Goodsell, D.S., Halliday, R.S., Huey, R., Hart, W.E., Belew, R.K. and Olson, A.J. (1998) J. Comput. Chem. 19, 1639–1662.
[23] Åqvist, J. and Luzhkov, V. (2000) Nature 404, 881–884.

[24] Luzhkov, V.B., Österberg, F., Acharaya, P., Chattopadhyaya, J. and Åqvist, J. (2002) Phys. Chem. Chem. Phys. 4, 4640–4647.

[25] Zwanzig, R.W. (1954) J. Chem. Phys. 22, 1420–1426.

[26] Kollman, P. (1993) Chem. Rev. 93, 2395–2417.

[27] Brandsdal, B.O., Österberg, F., Almlöf, M., Feiegberg, I., Luzhkov, V.B. and Åqvist, J. (2003) Adv. Prot. Chem., in press.

[28] Cornell, W.D., Cieplak, P., Bayly, C.L., Gould, I.R., Merz Jr., K.M., Ferguson, D.M., Spellmeyer, D.C., Fox, T., Caldwell, J.W. and Kollman, P.A. (1995) J. Am. Chem. Soc. 117, 5179–5197.

[29] Marelius, J., Kolmodin, K., Feierberg, I. and Åqvist, J. (1998) J. Mol. Graph. Model. 16, 213–225.

[30] Luzhkov, V.B. and Åqvist, J. (2000) Biochim. Biophys. Acta 1481, 360–370.

[31] Ryckaert, J.P., Cicotti, G. and Berendsen, H.J.C. (1977) J. Comput. Phys. 23, 327–341.

[32] Rao, B.G. and Singh, U.C. (1989) J. Am. Chem. Soc. 111, 3125–3133.

[33] Pearlman, D.A. and Kollman, P.A. (1991) J. Chem. Phys. 94, 4532–4544.

[34] Gough, C.A., Pearlman, D.A. and Kollman, P. (1993) J. Chem. Phys. 99, 9103–9110.

[35] Newland, C.F., Adelman, J.P., Tempel, B.L. and Almers, W. (1992) Neuron 8, 975–982.

[36] Naudin, C., Bonhomme, F., Bruneel, J.L., Ducasse, L., Grondin, J., Lassègues, J.C. and Servant, L. (2000) J. Raman Spectrosc. 31, 979–985.

[37] Alder, R.W., Allen, P.R., Anderson, K.R., Butts, C.R., Khosravi, E., Martin, A., Maunder, C.M., Orpen, A.G. and St. Pourçain, C.B. (1998) J. Chem. Soc. Perkin Trans. 2, 2083–2107.

[38] Berendsen, H.J.C., Postma, J.P.M., van Gunsteren, W.F., di Nola, A. and Haak, J.R. (1984) J. Chem. Phys. 81, 3684–3690.